Available online at www.sciencedirect.com
SCIENCE DIRECT®
Journal of Membrane Science 221 (2003) 185–197
journal of MEMBRANE SCIENCE
www.elsevier.com/locate/memsci

Gas sorption, permeation and separation of ABS copolymer membrane

José Marchese [a,*], Eduardo Garis [a], Marcia Anson [a], Nelio A. Ochoa [a], Cecilia Pagliero [b]

[a] *Laboratorio de Ciencias de Superficies y Medios Porosos, Dpto. de Química, UNSL-CONICET-FONCYT, Chacabuco, 915-5700 San Luis, Argentina*
[b] *GIDPO, Universidad de Río Cuarto, CONICET, Ruta 36-Rio Cuarto, Argentina*

Received 19 September 2002; received in revised form 1 May 2003; accepted 10 May 2003

Abstract

This work examines the gas transport and sorption properties of a commercial acrylonitrile–butadiene–styrene (ABS) copolymer (Lustran® 246), containing 60% styrene, 27% acrylonitrile and 13% butadiene. Permeability, diffusion and sorption coefficients of CO_2, CH_4, N_2 and O_2 in ABS membrane were determined at temperatures from 20 to 50 °C and pressures in the 2–10 × 10^5 Pa range. The coefficients correspond to the van't Hoff and Arrhenius relationships. In order to analyze the effect of plasticization, permeation properties were also determined at a feed pressure of 2 × 10^6 Pa with a 50% CO_2/CH_4 mixture. Interesting O_2 permeability values and O_2/N_2 separation factors in the whole range of temperature studied were obtained.

The results presented and discussed in this paper suggest that the ABS copolymer can be used as membrane material for the separation of O_2/N_2 at moderate temperature (20–50 °C), as far as it exhibits a balance of adequate thermal, mechanical and gas separation properties.

Keywords: ABS copolymer; Gas separation; Solubility; Permeability; Diffusivity

1. Introduction

Membrane technologies for gas separation have emerged as a viable alternative to conventional technologies such as cryogenics, catalytic and pressure swing adsorption. An important factor is to make a membrane process economically feasible, obtaining a highly permeable and selective membrane with good mechanical and thermal stability [1,2]. In the last two decades, remarkable progress has been made in the development of high-performance polymers for gas separation. In particular, glassy polymers (polysulfone, polyimide, polycarbonate, etc.) have been widely applied to the separation of gas mixtures such as oxygen/nitrogen and carbon dioxide/methane.

Considerable information is available on the dependence of permeability, diffusion and solubility coefficients for CO_2, CH_4, N_2 and O_2 on the structures of a variety of polycarbonates and polysulfone [3–8]. Polysulfone has satisfactory gas permeabilities and acceptable permselectivities and it can be used with highly sorbing plasticizing gases. These properties and its relative low cost set up polysulfone as a standard membrane material. Polycarbonates tend

* Corresponding author. Tel.: +54-2652-436151; fax: +54-2652-430224.
E-mail address: marchese@unsl.edu.ar (J. Marchese).

0376-7388/$ – see front matter © 2003 Elsevier B.V. All rights reserved.
doi:10.1016/S0376-7388(03)00258-8

to have comparable or higher permeabilities for light gases than analogous polysulfones, and both polymers have also comparable selectivities for O_2/N_2 and CO_2/CH_4 gas pairs.

Aromatic polyimide and polypyrrolone, which have high thermal and chemical resistances, exhibit an improved correlation between permeability and selectivity that make them prospective material for polymer membrane [9,10]. Polyimide is strongly affected by highly soluble penetrants, such as CO_2, plasticizing the polymer matrix [11]. Nevertheless, a comparison of analogous polycarbonates and polyimides, for example, polycarbonate and 6FDA–IPDA or HFPC and 6FDA–6FpDA, lead to higher CO_2 and O_2 permeabilities and higher O_2/N_2 and CO_2/CH_4 selectivities for polyimides [8].

A number of authors have developed various copolymers from known homopolymers as an alternative to the synthesis of entirely new polymers. The copolymer is intended to optimize the gas separation properties of the homopolymers, and in some cases also their mechanical properties. Stern et al. [12] reported that the gas permeation properties of copolymers depended on their chemical composition and morphology. Polyimides and related polymers, synthesized from aromatic reactants, have generally rigid-chain structures resulting in low gas permeability. To overcome the high rigidity of the polymer chains, block copolymers with incorporation of flexible segments such as siloxane [13] and ether linkage [14] have been studied. The incorporation of the siloxane unit to polyimides increases the solubility and permeability. A similar effect on polyimides and polypyrrolone has the introduction of an ester group in the polymer backbone [15]. Also the presence of a methyl group into the polyimide backbone leads to an increase in H_2, N_2 and O_2 permeability and permselectivity. Replacement of the rigid moiety of polyimide with a more flexible segment leads to an increase in permeability but with decreased permselectivity.

Recently Kim et al. [16] investigated the effect of the chemical composition and morphology of PEBAX® series copolymers on the permeation behavior of polar/nonpolar mixtures. PEBAX® is a block copolymer that combines a polymide block (hard segment or impermeable phase) and a polyether block (soft segment or permeable phase). They reported that PEBAX® copolymers show the highest permeability and selectivity for polar/nonpolar gas pairs (i.e. $\alpha_{CO_2/CH_4} = 61$, $\alpha_{SO_2/N_2} = 500$). For small and nonpolar gases (i.e. He, H_2, O_2 and N_2), the permeability decreases with increasing molecular size or volume. The high permeability and permselectivity of polarizable gases through this copolymer were attributed to their strong affinity to polyether block in PEBAX®.

The present work deals with dense gas separation membrane prepared from commercial acrylonitrile–butadiene–styrene (ABS) graft copolymer trademark Lustran®246. The reason of choosing ABS as a model copolymer is that Lustran®246 is a commercial material of relative low cost, with good balance of mechanical properties and moderate glass transition temperature (110 °C). The ABS material has rubbery segments (butadiene) dispersed in a glassy matrix (styrene-co-acrylonitrile). This chemical structure suggests that ABS would allow to obtain relative high permeation fluxes (rubbery region) and relative high separation factors (glassy matrix). Sorption and permeation of pure CO_2, CH_4, N_2 and O_2 through an appropriately manufactured ABS membrane were tested. The influence of both pressure and temperature on ABS separation and permeation properties will be discussed based on gas sorption and permeability data between 293 and 323 K and 2–10 $\times$ 10^5 Pa.

Since glassy polymers tend to produce plasticization by CO_2 it is important to determine the magnitude to which its presence in dense ABS membrane affects the comparison between mixed and pure gas permeation for the separation of CO_2 and CH_4. Permeabilities for binary 50:50 CO_2/CH_4 feed mixture were measured to discard the plasticization behavior induced by CO_2. An upstream partial pressure of 10^6 Pa was selected, either for CO_2 or CH_4, in order to compare with the pure gas results conducted up to these pressures.

2. Experimental

2.1. Materials

ABS copolymer, trade mark Lustran®246, was provided by Bayer (Argentina). Lustran®246 resin is a high-impact grade of ABS with a good balance of mechanical properties and impact strength for substrate application. The glass transition temperature of

Table 1
Penetrant physical properties

Penetrant	T_c (K)	T_b (K)	σ_{kt} (Å)	σ_{LJ} (Å)	V_c (cm^3/mol)
CO_2	304.2	194.5	3.30	4	94.0
CH_4	190.7	111.6	3.80	3.82	99.3
O_2	154.4	90.0	3.46	3.43	74.4
N_2	126.2	77.2	3.64	3.68	90.1

$T \cong 110\,^{\circ}C$ was determined by differential scanning calorimetry using a Mettler DSC 305 calorimeter at a heating rate of 10 °C/min between −50 and 300 °C. An approximate composition of ABS resin, 60% styrene, 27% acrylonitrile and 13% butadiene, was obtained from FTIR spectra using a Nicolet FTIR 5SxC, according to the technique given elsewhere [17].

The pure gases used for this study include carbon dioxide, methane, oxygen and nitrogen, since they provide information about several industrially pertinent separations. The purity of the pure gases was more than 99.5%. For mixed gas permeation measurements a 50% CO_2/CH_4 mixture was used. For the thermal conductivity calibration of the gas chromatograph several mol CO_2/CH_4 samples were used (10, 30, 50, 70%). All gases were supplied by Air Liquid (Argentina). The penetrant kinetic and Lennard–Jones diameters (σ_{kt}, σ_{LJ}), critical volume and temperature (V_c, T_c) and boiling temperature (T_b) are shown in Table 1.

2.2. Membrane preparation

Prior to processing, ABS was dried during 2 h at 85 °C in a desiccant dehumidifying hopper dryer. The ABS dried pellets were dissolved to 5% concentration in dichloromethane solvent (Cl_2CH_2). After filtration, the solution was cast onto a flat glass plate at room temperature. After complete solvent evaporation it was further dried in a vacuum oven (50 °C, 0.5 atm) for 2 days to remove all detectable traces of the casting solvent. The membrane thickness was between 35 and 45 μm.

2.3. Equilibrium gas sorption

Equilibrium sorption of pure gas by ABS was measured by the pressure decay method [18]. The equipment consists basically of two chambers A and B, with well-known volumes, separated by a valve. The polymer sample, in the form of a thin wafer, was placed in the volume B and the gas under study was laid up to the chamber A at the desired pressure. After this, valve was opened for a short time to allow gas into the sample chamber. Sorption isotherms were measured using interval experiments, which successively increased the penetrant pressure. When equilibrium was reached, the amount of sorbed gas was calculated from the difference between the initial and final pressure in the sample chamber according to the ideal gas law.

2.4. Pure and mixture gas permeabilities

Permeation tests were performed with a modified time-lag apparatus similar to those described elsewhere in detail [19,20]. The effective membrane area was 19.64 cm^2 and permeate constant volume was 36.4 cm^3.

The amount of gas transmitted at time t through the ABS membrane was calculated from the permeate pressure (p_2) readings in the low-pressure side. The inherent leak rate in the downstream side determined after evacuating the system, was measured for each experimental run. Permeability constants (P) were obtained directly from the flow rate into the downstream volume upon reaching the steady state as

$$P\,(\text{Barrer}) = 6.65\frac{l}{T_c p_1}\frac{\mathrm{d}p_2}{\mathrm{d}t} \tag{1}$$

where $\mathrm{d}p_2/\mathrm{d}t$ is in cmHg/s, membrane thickness l is in cm.

For mixed gas permeation experiments, 50:50 CO_2/CH_4 at 2×10^6 Pa was used as the upstream feed. Permeate to feed flow rate ratio, which is the stage cut, was always less than 1%. Under these conditions, the residue composition was essentially equal to the feed solution. Concentration analysis was performed with the gas chromatograph GC-8APT from Shimadzu Corporation, equipped with a Carbopack C/HT column, thermal conductivity detector and a data processor Chromatopac C-R3A. Permeabilities and separation factors were calculated using average upstream and downstream compositions from at least six gas chromatograph measurements. The permeability coefficients of permeant i were calculated from the relationship

$$P_i = \frac{x_{ip} J l}{p_1 x_{if} - p_2 x_{ip}} \tag{2}$$

where x_{ip} and x_{if} are the molar fractions of the gas component i in the permeate and feed streams, respectively, J the total permeate flux (cm^3(STP)/cm^2 s), and p_1 and p_2 are the total pressures (cmHg) on the feed and permeate side of the membrane.

3. Results and discussion

3.1. Pressure and temperature dependence on sorption

Sorption measurements on ABS were made for each gas in the temperature range of 20–50 °C and equilibrium pressures between 2–15 × 10^5 Pa. Figs. 1 and 2 show the representative sorption isotherms for CO_2 and O_2. The sorption isotherms for CO_2 and CH_4, as usual for most gases in glassy polymers, tend to have concave shapes. Here this effect is especially relevant at pressures under 3 atm. The O_2 and N_2 isotherms are practically linear in all the range of pressure and temperature studied.

In the framework of glassy polymers the concept of two sites or two energy levels of dissolution are named as dual-sorption model. In this case it has been suggested that the total concentration of gas adsorbed (C) is described by the following equation [21]:

$$C = Sp + \frac{C'_H bp}{1 + bp} \quad (3)$$

which is a sum of Langmuir and Henry's law contributions, and where p is the partial pressure of the gas, S the Henry's dissolution constant, and b and C'_H are the hole affinity and the hole saturation constant.

Since we are only interested to analyze the thermodynamic parameter S, the Eq. (3) is approached to a linear asymptote at high pressures, which has an average solubility coefficient from the slope according to

$$C = \bar{S}p + C'_H \quad (4)$$

The apparent solubility coefficients, $\bar{S}$, obtained by linear least squares regression analysis of the solubility data are shown in Table 2. It is evident that the nature of the gas shows an important influence on ABS solubility. In effect, the solubility of CO_2 is roughly 4–5 times bigger than methane, 6–9 times than oxygen and 11–15 times than nitrogen. This selective solubility effect of CO_2 could be attributed to the presence of acrylonitrile in ABS copolymer. This assumption is in agreement with the results of Van Krevelen [22], who found a pronounced selective effect of the polymer polarity on gas solubility in butadiene–acrylonitrile copolymers. As the acrylonitrile content of the copolymer increases, the solubility of carbon dioxide increases, whereas that of nitrogen and oxygen decreases. Fig. 3 shows the representative linear behavior between the gas solubility in ABS

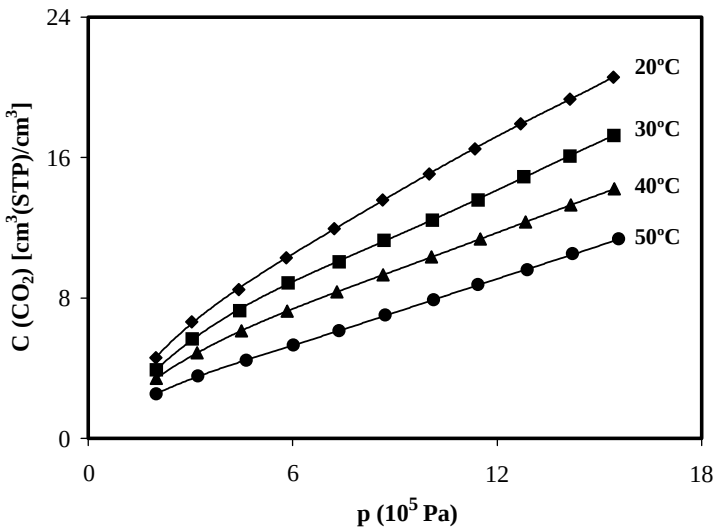

Fig. 1. CO_2 sorption isotherms from 20 to 50 °C in ABS copolymer membrane.

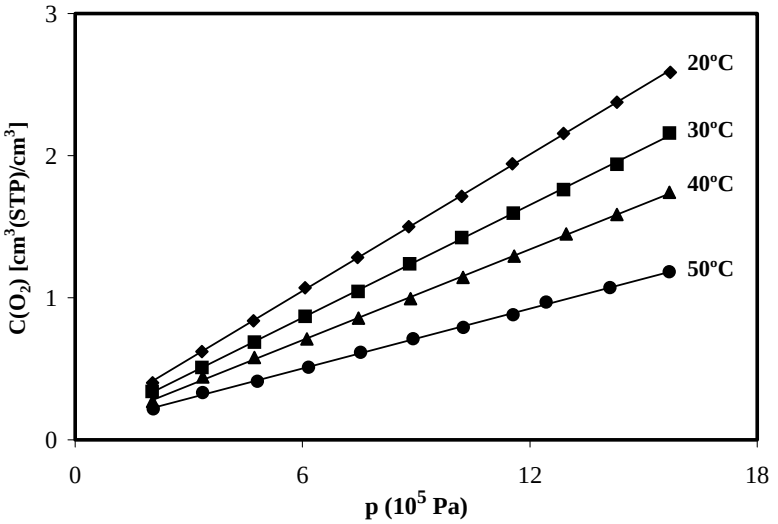

Fig. 2. O_2 sorption isotherms from 20 to 50 °C in ABS copolymer membrane.

Table 2
Apparent sorption, permeability and diffusivity parameters for the different penetrant/ABS systems

T (K)	$\bar{S} \times 10^5$ (cm^3(STP)/cm^3 Pa)				$\bar{P} \times 10^{10}$ (cm^3(STP)/cm^2 cmHg s)				$\bar{D} \times 10^8$ (cm^2/s)			
	CO_2	CH_4	O_2	N_2	CO_2	CH_4	O_2	N_2	CO_2	CH_4	O_2	N_2
293	1.07	0.26	0.16	0.09	2.97	0.126	0.697	0.103	2.11	0.363	3.33	0.889
303	0.91	0.21	0.13	0.08	3.57	0.175	0.950	0.162	2.98	0.624	5.51	1.590
313	0.74	0.17	0.11	0.06	3.97	0.248	1.240	0.210	4.08	1.080	8.89	2.870
323	0.63	0.14	0.08	0.04	4.95	0.355	1.550	0.264	5.95	1.930	14.5	4.580

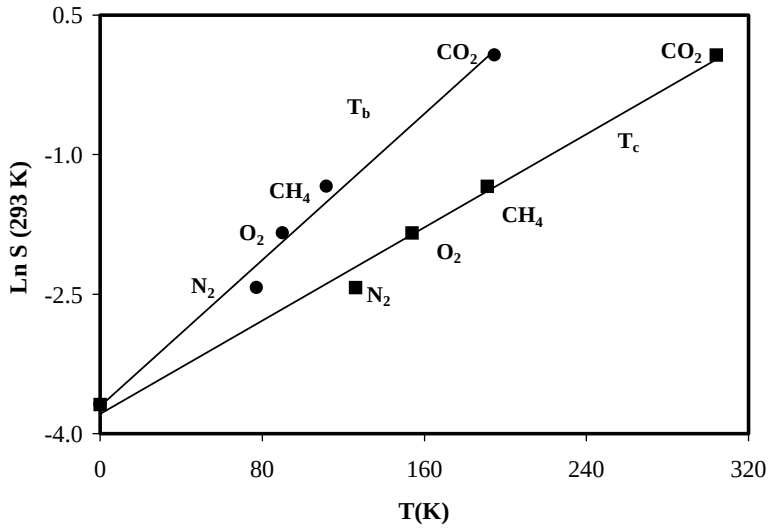

Fig. 3. Solubility of gas in ABS membrane as a function of the critical temperature an the boiling point of the gas.

Table 3
Parameter values from fitting the straight lines of $\ln S$ vs. T_b and T_c at different operational temperatures (T)

T (K)	Parameters from Eq. (5)			Parameters from Eq. (6)		
	a	b	R^2	c	d	R^2
293	−3.743	0.0199	0.970	−4.016	0.0136	0.990
303	−3.909	0.0199	0.981	−4.174	0.0135	0.996
313	−4.230	0.0206	0.966	−4.514	0.0140	0.987
323	−4.541	0.0213	0.972	−4.832	0.0145	0.992

($T = 293$ K) and their boiling points or their critical temperatures. The plot shows that the gas solubility depends on the inherent condensability of the respective gases. This behavior is typical for simple gas sorption in amorphous polymers without strong polar groups. In this case the drawn lines can be described by the following general expressions:

$$\ln S(T) = a + bT_b \tag{5}$$

$$\ln S(T) = c + dT_c \tag{6}$$

Parameters a, b, c, and d calculated by fitting the straight lines of $\ln S$ at different experimental temperatures versus T_b or T_c are summarized in Table 3. Eqs. (5) and (6) and these parameters may be useful as a first approximation to evaluate ABS solubility factor for other inorganic and organic gases such as: He, H_2, CO, SO_2, NH_3, C_2H_6, C_2H_4, C_3H_6, etc.

The temperature dependence of the average solubility coefficient obeys the van't Hoff equation

$$\bar{S} = S_0 \exp\left(-\frac{H_s}{RT}\right) \tag{7}$$

where S_0 is the pre-exponential factor and H_s is the heat of sorption. The van't Hoff plots of gas solubility coefficients in ABS are shown in Fig. 4 and the thermodynamic parameters determined from the linear regression are shown in Table 4. As expected, H_s values are negative indicating that the gas sorption in ABS is an exothermic process. From thermodynamic considerations, the most negative heats of sorption would be expected for the penetrants with the highest critical temperatures. However, the estimated H_s values tabulated in Table 4 ($CO_2 > CH_4 > N_2 > O_2$) do not follow this trend ($N_2 > O_2 > CH_4 > CO_2$ according to Table 1). Zimmerman and Koros [23] found the same behavior in their studies of gas sorption in the ladder polymer BBL. Like these authors, we account from these deviations by considering that the heat of sorption, H_s, is the sum of the negative enthalpy associated with gaseous condensation, H_c, and the positive enthalpy of mixing, H_m. In this case, it is suggested that the largest molecular volume of CH_4 and CO_2, respectively (see Table 1), would require a larger heat

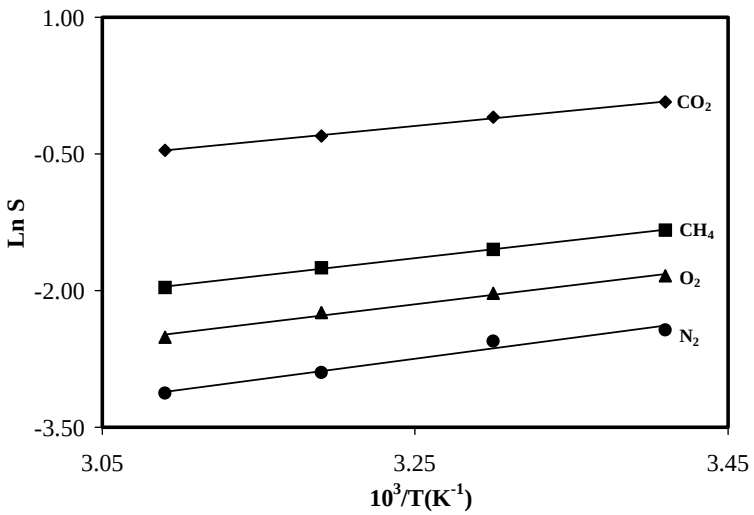

Fig. 4. Temperature dependence of gas solubility coefficients in ABS membrane.

Table 4
van't Hoff and Arrhenius parameters for the different penetrant/ABS systems

Penetrant	E_p (kcal/mol)	P_0 (cm^3(STP)/cm^2 cmHg s)	H_s (kcal/mol)	$S_0 \times 10^5$ (cm^3(STP)/cm^3 Pa)	E_d (kcal/mol)	D_0 (cm^2/s)
CO_2	3.11	6.10E−8	−3.33	3.55E−3	6.36	1.15E−3
CH_4	6.58	9.96E−7	−3.88	3.37E−4	10.31	1.74E−1
O_2	5.11	4.49E−7	−4.12	1.37E−4	9.08	1.93E−1
N_2	5.91	2.76E−7	−4.52	3.95E−5	10.24	3.83E−1

of mixing which in turn would increase the heat of sorption.

3.2. Pressure and temperature dependence on permeability and diffusivity

As mentioned, transport parameters for single gases were calculated from permeation experiments by the time-lag method. Measurements were made for each system at four different temperature levels in the range 20–50 °C, and in the feed pressure range from 2×10^5 to 10^6 Pa. The calculated permeability values for CO_2, N_2, O_2 and CH_4 are presented in Figs. 5 and 6. From these results it is evident that the upstream gas pressure or gas concentration in the range proposed has no significant effect on the gas permeabilities. The results also reveal the general behavior in which gas permeation rate is enhanced with increasing temperature. The average values of pure gas permeabilities in ABS are summarized in Table 2.

Fig. 5 also compares the permeabilities for CO_2 and CH_4 in the pure and mixed gas experiments at 10 atm and different temperatures. In all cases the mixed gas results are identical with those for the pure gases within the experimental accuracy of the measurements. Thus, it can be considered that until a partial pressure of 10 atm for CO_2 and for CH_4 the effects of site competition or plasticization seem to be entirely negligible for these systems. These results allow us to assume that, in the experimental conditions analyzed, the mixed CO_2/CH_4 gas permeation behavior in ABS membrane can be adequately predicted by pure gas measurements.

The permeation of a nonporous polymeric membrane by a penetrant gas is generally considered to be a solution–diffusion process [24]. According to this mechanism, gas permeation is a complex process that involves the sorption of the penetrant in the polymeric film, followed by a diffusion of gas molecule across the membrane matrix due to a concentration gradient.

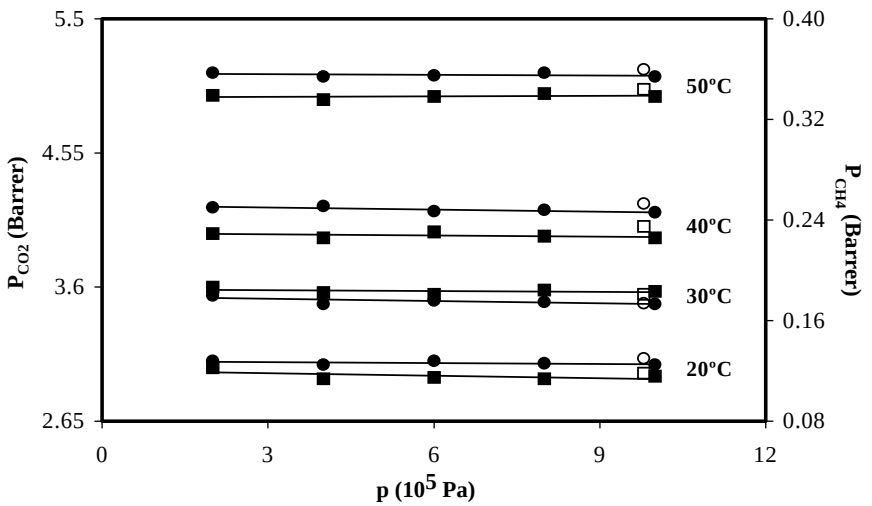

Fig. 5. CO_2 (■) and CH_4 (●) permeation isotherms for pure gases and 50:50 CO_2/CH_4 gas mixture at 2×10^6 Pa, CO_2 (□)/CH_4 (○).

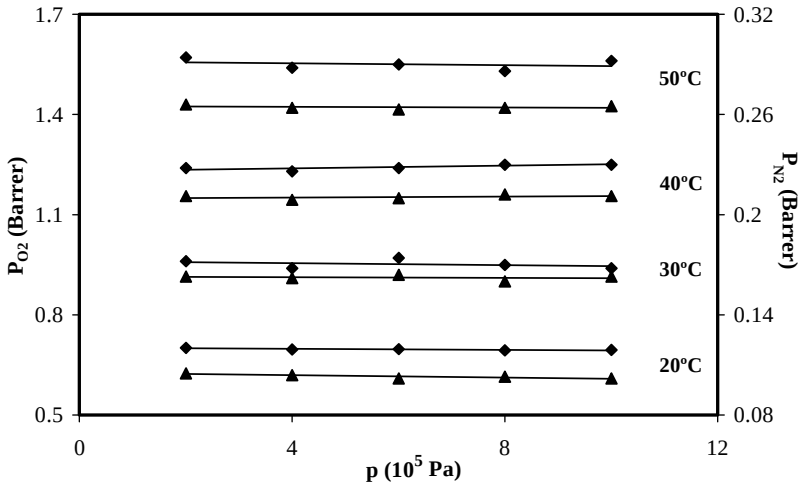

Fig. 6. O_2 (◆) and N_2 (▲) gas permeation isotherms.

Many CO_2-glassy polymer transport measurements from time-lag technique have shown that the magnitude of the upstream pressure (p_1) could have some significant effect on the gas permeability. Paul and Koros [25] have interpreted this behavior with the dual mobility, or partial immobilization model. The permeability expression is given by

$$P = SD + \frac{D_H C'_H b}{1 + bp_1} \tag{8}$$

where D and D_H are the diffusion coefficients in the Henry's law portion and in the Langmuir portion, respectively. The relatively small or negligible p_1 dependence of permeability between 2–10 $\times 10^5$ Pa for our systems may be ascribed to a very high (or complete) immobilization of the Langmuir population ($D_H/D \cong 0$) or to a saturation of the Langmuir environments, with the permeation occurring primarily in the Henry region. In this case, the permeability parameter defined in Eq. (8) could be expressed simply as the product of the apparent solubility coefficient and the apparent diffusion coefficient ($\bar{D}$) in the pressure range studied as follows:

$$\bar{P} = \bar{S}\bar{D} \tag{9}$$

The apparent diffusion coefficients evaluated from Eq. (9) for each gas/ABS system and temperature are given in Table 2. Gas diffusion in polymeric membranes can be considered as an activated process and the temperature dependence of the diffusion coefficients may be described using an Arrhenius-type expression as follows:

$$\bar{D} = D_0 \exp\left(-\frac{E_d}{RT}\right) \tag{10}$$

where E_d is the activation energy for diffusion and D_0 is a pre-exponential factor.

The effect of temperature on gas permeability can be expressed by a combination of Eqs. (7), (9) and (10) as follows:

$$\bar{P} = P_0 \exp\left(-\frac{E_p}{RT}\right) \tag{11}$$

where $P_0 = S_0 D_0$ is the pre-exponential factor and $E_p = E_d + H_s$ is the apparent activation energy for permeation. Eqs. (7), (10) and (11), of course, are only valid within temperature ranges that do not include significant thermal transitions of the polymer.

To illustrate the ability of Eq. (11) to characterize the experimental data, Arrhenius plots are represented in Fig. 7 showing straight lines with high correlation coefficients. Having established the validity of Eq. (11) within the temperature range of 20–50 °C, the Arrhenius parameters for permeation of CO_2, CH_4, N_2 and O_2 calculated by fitting the straight lines are summarized in Table 4. Fig. 8 illustrates the predicted Arrhenius temperature dependence of gas diffusivity coefficients generated from the gas permeation and solubility data (Table 2). The activation

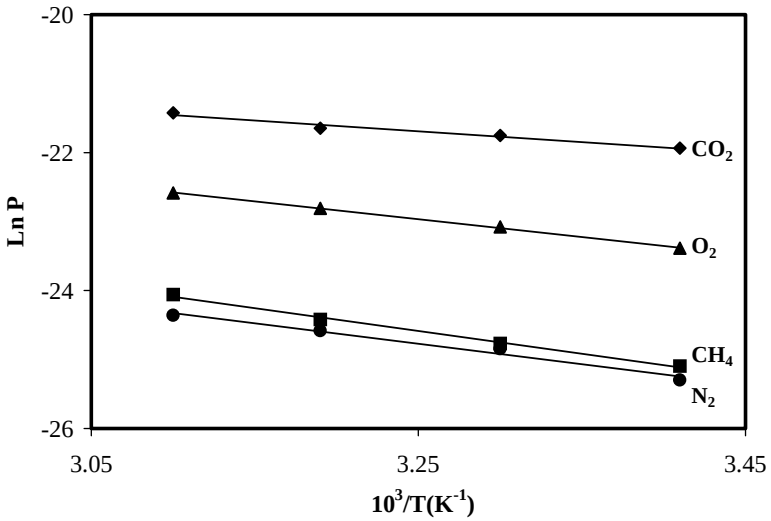

Fig. 7. Temperature dependence of gas permeability coefficients in ABS membrane.

energies for diffusion are shown in Table 4, along with their corresponding pre-exponential factors.

The activation energies for permeation follow the expected trends, as far as they increase with the penetrant kinetic diameter. The very low E_p value of CO_2 compared with those of O_2, N_2 and CH_4, could be attributed primarily to the lower heat consumption for CO_2 diffusion, lowering the amount of energy associated with permeation. Also, the diffusion activation energies increase with the penetrant kinetic diameter. However, it is clear from Tables 1 and 2 that there is no correlation between the CO_2/O_2 diffusion coefficients ($D_{CO_2} < D_{O_2}$) and their kinetic diameters ($\sigma_{kt(CO_2)} < \sigma_{kt(O_2)}$).

Tanaka et al. [26] have examined the permeation of hydrocarbon gases, CO, CO_2, CH_4 and N_2 in 6FDA polyimides and PPO. In their work a good correlation of the diffusion coefficient on the gas effective

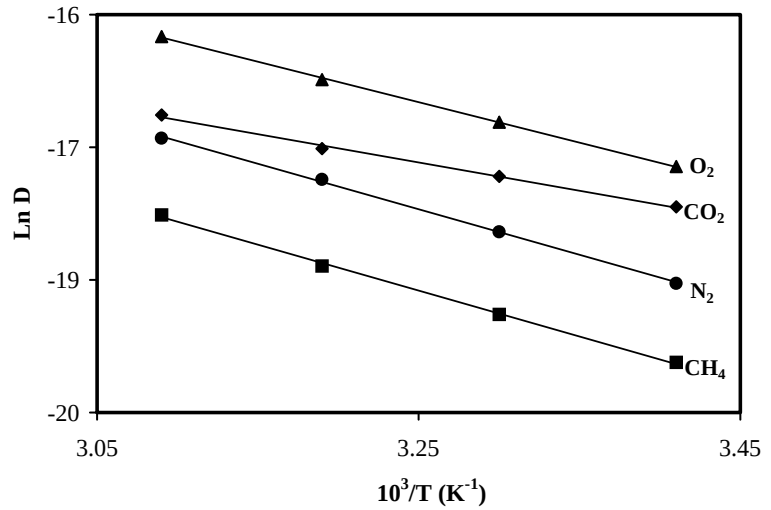

Fig. 8. Temperature dependence of gas diffusivity coefficients in ABS membrane.

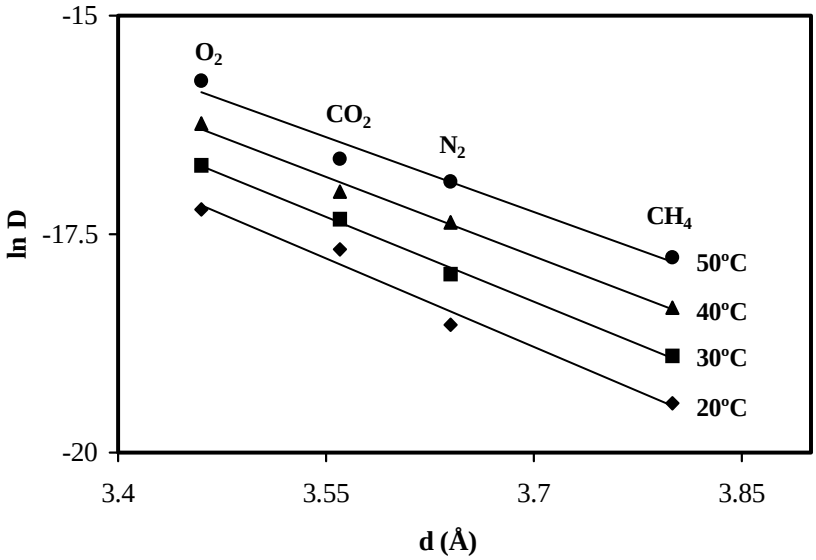

Fig. 9. Correlation of diffusion coefficients with kinetic diameter and critical volume of the penetrants in ABS membrane.

diameter (d) was obtained. In their analysis, the collision diameter of Lennard–Jones potential was considered as effective diameter for diffusion for all the hydrocarbon gases, whereas a value of $d = 3.5$ Å for CO_2 was used based on a good correlation between D and d of these gases for various polymers [27,28]. For O_2, N_2 and CH_4 the difference in the magnitude between σ_{kt} and σ_{LJ} is negligibly small and both were equally adequate as effective diameter. Fig. 9 shows the linear dependence of the ABS diffusion coefficient on the gas effective diameter at different temperatures. In this plot an average $d(CO_2) = 3.56$ Å was used as obtained from linear correlations of $\ln D$ and d (or σ_{LJ}) of O_2, N_2 and CH_4 at different temperatures. Good concordance between our effective diameter value for CO_2 and Tanaka's one has been obtained. Nevertheless the deep reasons why this effective diameter has to be used for CO_2 remain undefined.

Other possible explanation of this behavior could be in terms of both the kinetic diameter and its molecular volume. The activation energy for diffusion (E_d) is a measure of how difficult is for the molecule to jump from a site or hole to another hole. The kinetic diameter, which in fact corresponds to the minimum molecular diameter, will have a strong effect on the penetrant mobility. It is evident that if the penetrant kinetic diameter was small, its mobility through the polymer gaps should be higher with smaller activation energy. On the contrary, larger holes need to be formed in the polymer for the diffusion of larger molecules, hence the activation energy will be larger for the diffusion of bigger molecules and the diffusivity will be smaller. A tentative possibility to take into account the effect of both the kinetic aspect of the barrier and the possibility of the polymer to accommodate big molecules could be the product $\sigma_{kt}V_c$. Fig. 10 shows the diffusivity as a function of ($\sigma_{kt}V_c$) for the different molecules. While this correlation is intuitively satisfying, it certainly oversimplifies the actual differences in molecular-scale environments sampled by a penetrant as it moves through the polymer.

3.3. Temperature dependence of selectivity

The overall permselectivity of polymer membrane toward two different penetrant gases i and j is commonly expressed in terms of an ideal separation factor, α_{ij}, which is defined by the relation, cf. Eq. (9):

$$\alpha_{ij} = \frac{\bar{P}_i}{\bar{P}_j} = \left(\frac{\bar{D}_i}{\bar{D}_j}\right)\left(\frac{\bar{S}_i}{\bar{S}_j}\right) = \alpha_{ij}^{D}\alpha_{ij}^{S} \tag{12}$$

where α_{ij}^{D} and α_{ij}^{S} indicate the mobility for diffusivity-selectivity and the solubility-selectivity, respectively.

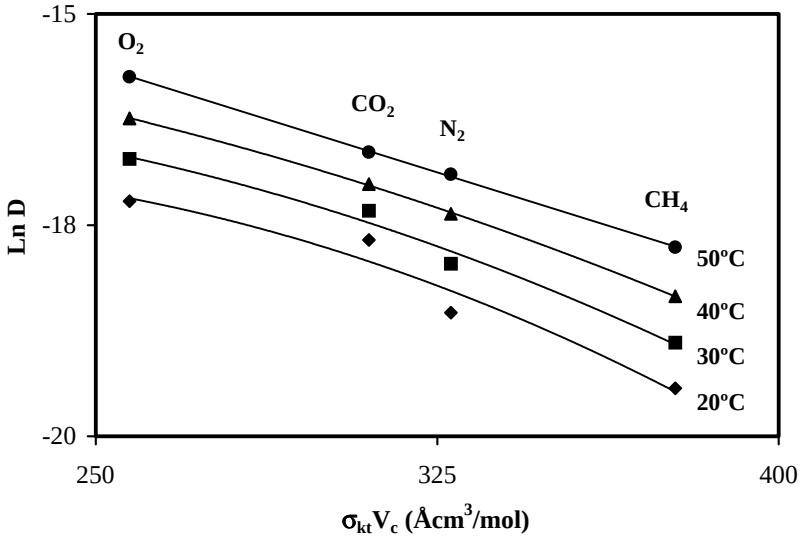

Fig. 10. Correlation of diffusion coefficients with effective diameter of the penetrants in ABS membrane.

It follows from Eq. (12) that the relative effects of temperature on selectivity for CO_2/CH_4 and O_2/N_2 separations trough the ABS membrane can be found by taking the ratio of Eq. (11) or Eqs. (7) and (10) for each pair of components and the data of Table 4, that is

$$\alpha_{(CO_2/CH_4)} = 6.12 \times 10^{-2} \exp\left(\frac{1750.6}{T}\right), \qquad \alpha_{(O_2/N_2)} = 1.63 \exp\left(\frac{406.4}{T}\right) \tag{13}$$

$$\alpha^{D}_{(CO_2/CH_4)} = 6.65 \times 10^{-3} \exp\left(\frac{1988.5}{T}\right), \qquad \alpha^{D}_{(O_2/N_2)} = 0.5 \exp\left(\frac{584.3}{T}\right) \tag{14}$$

$$\alpha^{S}_{(CO_2/CH_4)} = 10.53 \exp\left(-\frac{277.7}{T}\right), \qquad \alpha^{S}_{(O_2/N_2)} = 3.49 \exp\left(-\frac{200.1}{T}\right) \tag{15}$$

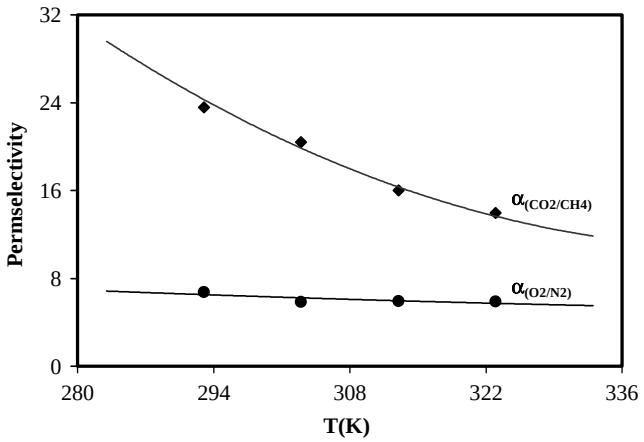

Fig. 11. Temperature dependence of experimental values and theoretical correlation (from Eq. (13), solid lines) of ABS permselectivities.

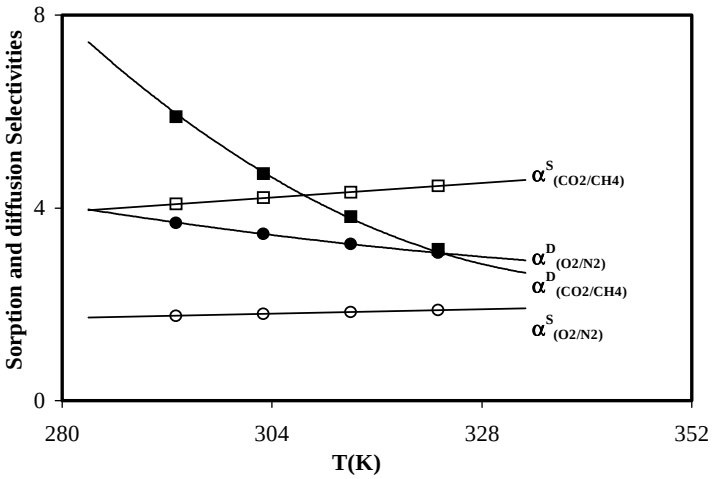

Fig. 12. Temperature dependence of experimental values and theoretical correlation (from Eqs. (14) and (15), solid lines) of ABS solubility and diffusivity selectivities.

The temperature dependence of ABS permselectivity for two gas separations according to Eq. (13), and experimental separation factors for the corresponding gas mixtures are shown in Fig. 11. This figure shows the good correlation between the theoretical and experimental selectivity values. In Fig. 12 the values of ideal diffusivity and solubility separation factors are plotted against the temperature. An examination of Figs. 11 and 12 indicates that both the pronounced decline in CO_2/CH_4 and the slight decrease of O_2/N_2 permeability with increasing temperature may be attributed to the decreased diffusivity ratios, since solubility-selectivities increase slightly with the increasing temperature.

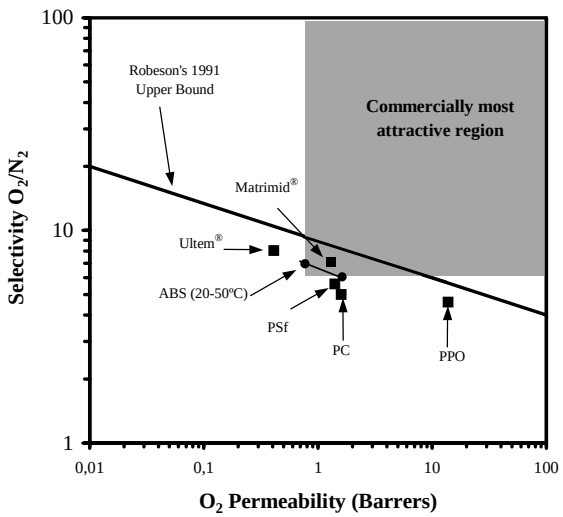

Fig. 13. Comparison of O_2/N_2 separation performance for ABS copolymer (20–50 °C) and various traditional polymeric materials (35 °C) used in gas separation membrane.

The ABS membrane shows interesting O_2/N_2 and CO_2/CH_4 permselectivities. In particular, the adequate values of O_2 permeabilities for the ABS membrane (0.7 Barrer at 20 °C and 1.6 at 50 °C) along with the relatively high O_2/N_2 permselectivities (6.8 at 20 °C and 5.9 at 50 °C) make this polymeric material a competitive candidate for use in moderated temperature O_2/N_2 gas separation membrane. A comparison of O_2/N_2 separation performance for ABS copolymer with other traditional polymeric material used in gas separation membrane is shown in Fig. 13. The solid line in this figure is the trade-off between O_2 permeability and O_2/N_2 selectivity [29]. The plot of ABS permselectivities between 20 and 50 °C fell in the desired range for practical applications.

4. Conclusions

In this study, a thorough analysis of the effect of temperature and pressure on the transport, sorption and selective properties of the ABS membrane is provided. Dense ABS membrane from Lustran®246 resin

copolymer were prepared and tested for O_2, N_2, CO_2, and CH_4 permeabilities. The influence of temperature (20–50 °C) and pressure ($2–10 \times 10^5$ Pa) on gas permeability through dense ABS membranes has been studied.

Sorption isotherms for pure gases in ABS membrane at 20, 30, 40 and 50 °C show the typical behavior of simple gas sorption in amorphous polymers without strong polar groups. The higher CO_2 solubility was attributed to the presence of acrylonitrile segment in the ABS copolymer. The CO_2 and CH_4 permeabilities from CO_2/CH_2 mixture were identical to those obtained from pure gases, indicating that until a pressure of 10^6 Pa for CO_2 the effect of plasticization appears to be negligible for CO_2/ABS system. Interesting permeability values and ideal separation factors (O_2/N_2, CO_2/CH_4) in the whole range of temperature were obtained. The O_2/N_2 ideal selectivities are among the highest reported by other authors using traditional membrane materials.

References

[1] M. Mulder, Basic Principles of Membrane Technology, Kluwer Academic Publishers, Dordrecht, 1991.

[2] R.E. Kesting, A.K. Fritzsche, Polymer Gas Separation Membranes, Wiley, New York, 1993.

[3] A.J. Erb, D.R. Paul, Gas sorption and transport in polysulfone, J. Membr. Sci. 8 (1981) 11.

[4] I. Pinnau, W.J. Koros, Structures and gas separation properties of asymmetric polysulfone membranes made by dry, wet, and dry/wet phase inversion, J. Appl. Polym. Sci. 43 (1991) 1491.

[5] J. Marchese, C.L. Pagliero, Characterization of asymmetric polysulfone membranes for gas separation, Gas Sep. Purif. 5 (1991) 215.

[6] J.C. Schimdhauser, K.L. Longley, The effect of bisfenol monomer structure on gas permeability of aromatic polycarbonates, J. Membr. Sci. 39 (1991) 2083.

[7] C.L. Ailken, D.R. Paul, Gas transport properties of polysulfones based on dihydroxynaphthalene isomers, J. Polym. Sci., Part B: Polym. Phys. 31 (1993) 1061.

[8] W.J. Koros, D.R.B. Walker, Gas separation membrane material selection criteria: weakly and strongly interacting feed component situations, Polym. J. 23 (1991) 481.

[9] S.A. Stern, Polymers for gas separation: the next decade, J. Membr. Sci. 94 (1994) 1.

[10] L.M. Costello, D.R.B. Walker, W.J. Koros, Analysis of a thermally stable polypyrrolone for high temperature membrane-based gas separations, J. Membr. Sci. 90 (1994) 117.

[11] W.J. Koros, M.R. Coleman, D.R.B. Walker, Controlled permeability polymer membranes, Ann. Rev. Sci. 22 (1992) 47.

[12] S.A. Stern, V.M. Shah, B.J. Hardy, Structure–permeability relationships in silicone polymers, J. Polym. Sci., Polym. Phys. Ed. 25 (1987) 1263.

[13] Y.B. Lee, H.B. Park, J.K. Shim, Y.M. Lee, Synthesis and characterization of polyamideimide-branched siloxane and its gas-separation, J. Appl. Polym. Sci. 74 (1999) 965.

[14] K. Okamoto, M. Fujii, S. Okamyo, H. Suzuki, K. Tanaka, H. Kita, Gas permeation properties of poly(ether imide) segmented copolymers, Macromolecules 28 (1995) 6950.

[15] G. Xuesong, L. Fengcai, Gas transport properties of polyimides and polypyrrolone containing ester linkage, Polymer 36 (1995) 1035.

[16] J.H. Kim, S.Y. Ha, Y.M. Lee, Gas permeation of poly(amide-6-*b*-ethylene oxide) copolymer, J. Membr. Sci. 190 (2001) 179.

[17] J. Haslam, H. Willis, D.C. Squirrel, Identification and Analysis of Plastics, Wiley, New York, 1983.

[18] W.J. Koros, D.R. Paul, A.A. Rocha, Carbon dioxide sorption and transport in polycarbonate, J. Membr. Sci. 14 (1976) 687.

[19] S.S. Dhingra, E. Marand, Mixed gas transport study through polymeric membranes, J. Membr. Sci. 141 (1998) 45.

[20] P.C. Raymond, W.J. Koros, D.R. Paul, Comparison of mixed and pure gas permeation characteristics for CO_2 and CH_4 in copolymers and blends containing methyl methacrylate units, J. Membr. Sci. 77 (1993) 49.

[21] W.R. Vieth, M.A. Amini, in: H.B. Hopfenberg (Ed.), Permeability of Plastic Films and Coatings to Gases, Vapors, and Liquids, Plenum Press, New York, 1974, p. 49.

[22] D.W. Van Krevelen (Ed.), Permeation of polymers—the diffusive transport of gases, vapors and liquids in polymers, in: Properties of Polymers, Elsevier, Amsterdam, 1976, pp. 403–425.

[23] C.M. Zimmerman, W.J. Koros, Comparison of gas transport and sorption in the ladder polymer BBL and semi-ladder polymers, Polymer 40 (1999) 5655.

[24] W.J. Koros, G.K. Fleming, Membrane based gas separation, J. Membr. Sci. 83 (1993) 1.

[25] D.R. Paul, W.J. Koros, Effect of partially immobilizing sorption on permeability and the diffusion time lag, J. Polym. Sci., Polym. Phys. Ed. 14 (1976) 675.

[26] K. Tanaka, A. Taguchi, J. Hao, H. Kita, K. Okamoto, Permeation and separation properties of polyimide membranes to olefins and paraffins, J. Membr. Sci. 121 (1996) 197–207.

[27] K. Okamoto, M. Fujii, S. Okamyo, H. Suzuki, K. Tanaka, H. Kita, Gas permeation properties of poly(ether imide) segmented copolymers, Macromolecules 28 (1995) 6950.

[28] K. Okamoto, K. Tanaka, H. Kita, M. Ishida, M. Kakimoto, Y. Imai, Gas-permeability of polyimides prepared from 4,4′-diaminotriphenylamine, Polym. J. 24 (1992) 451.

[29] L.M. Robenson, Correlation of separation factor versus permeability of polymeric membranes, J. Membr. Sci. 62 (1991) 165.